PHY 122B Cosmic Microwave Background Lab Report

Guanyu Qian
University of California, Davis

May 11th 2022

Abstract

This experiment is designed to study the cosmic microwave background radiation using a radiometer connected with an amplifier and passive filters. This is an important experiment because CMB is produced at the universe's beginning. Measuring its magnitude discloses the evolution of the universe. The overall methodology used is to point a microwave horn to the sky to capture 19GHz radiation and vary its angle relative to the zenith while recording the power the antenna received. The experiment is repeated five times to acquire a higher precision. In data analysis, the line fit of temperature observed versus airmass is plotted using five data trials to obtain the CMB temperature. The result is T_{cmb}= 1.7K $\pm$ 0.4K (random) $\pm$ 1.3K (syst). Although it is around 1K difference from the published value, this experiment verifies the existence of cosmic microwave background radiation.

1 Introduction

Cosmic microwave background, CMB, originates from the beginning of the universe's formation, which is also known as the Big Bang theory. CMB is also one of the most ancient forms of energy that humans can observe. Therefore, measuring its magnitude can potentially unveil the progress of how the universe has evolved. The measurement of CMB has become an inevitable problem for experimental physicists to solve to understand the evolution of the universe.

1.1 Formation of Cosmic Microwave Background

The cosmic microwave background radiation is caused by the photon generated in the decoupling process. At the beginning of the Big Bang, the universe was a fireball plasma, meaning that it had a high temperature and a large density, giving rise to massive radiation. As shown in Fig 1, protons and electrons could not be recombined because they possessed high energy, making them extremely unstable. As the fireball started to expand and cool down, the protons

and electrons recombined and generated photons, as shown in the right part of Fig 1. After 300000 years, the universe was around 3000 Kelvin, and it became transparent for the photons to move. Thus, they kept traveling in the universe up till the present moment. Due to the Doppler effect, photons experienced a redshift, and their magnitude decreased by a factor of 1100. Nowadays, the published CMB temperature is 2.725K.

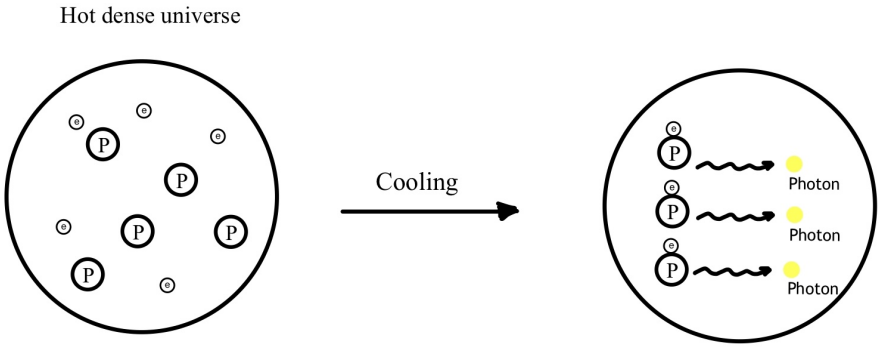

Figure 1: The fireball plasma is shown on the left. The electrons and protons could not recombine because they possess high energy, which makes them extremely unstable. As the fireball cooled down, the electrons and protons could be recombined to form matters. In this process, photons were generated, contributing to the cosmic background radiation, as shown on the right.

1.2 Intensity and Temperature Measurements

The cosmic microwave background temperature is not directly measured in this experiment, while the intensity is measured using the power meter. However, Plank's Law offers the relationship between intensity and temperature, which can be applied to derive the temperature of the cosmic microwave background.

$$I_v(T) = \frac{2hv^3}{c^2} * \frac{1}{e^{hv/kT} - 1} \tag{1}$$

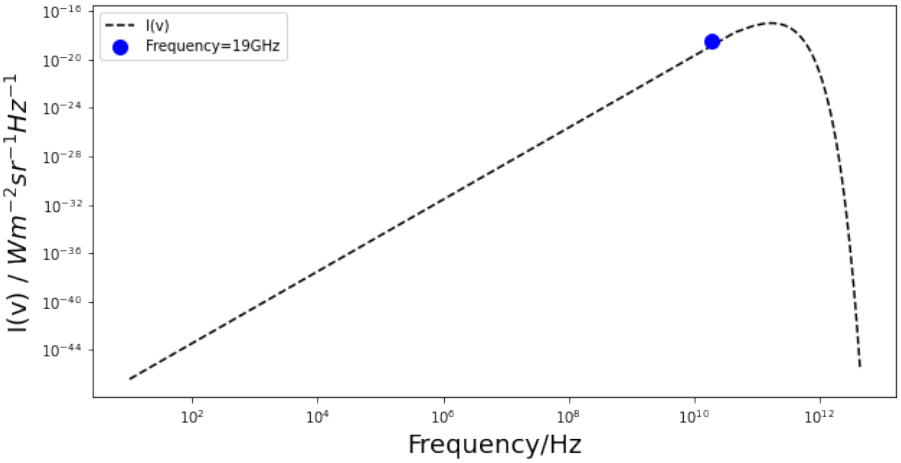

Figure 2: This is the I_v plot for Plank's Law where T= 2.725K which is the approximation of the CMB temperature. In this experiment, the radiometer receives 19 GHz radiation from the sky. Therefore, the point of interest is f=19 GHz which is marked by blue in the plot.

As shown in Fig 2, the point of interest, f=19 GHz, is located in the linear region of Plank's Law. The linear approximation of Plank's Law is derived from the Rayleigh-Jeans limit where kT $\gg$ hv.

$$e^{hv/kT} \approx 1 + \frac{hv}{kT} \tag{2}$$

Plank's Law is simplified into a linear relationship combining Eqn 1 and Eqn 2.

$$I_v(T) = \frac{2kTv^2}{c^2} \tag{3}$$

This linear relationship only applies when the temperature is larger than frequency (in GHz) /20 due to Rayleigh-Jeans limit. In this experiment, $\frac{19(GHz)}{20} <$ 2.725 (approximation of the black body temperature). Therefore, 19 GHz with 500 MHz interval works within the linear region of the Planck's Law. This assumption makes sure that the CMB temperature can be predicted using a linear line fit in the data analysis. The linear approximation of Plank's Law is shown in Fig 3.

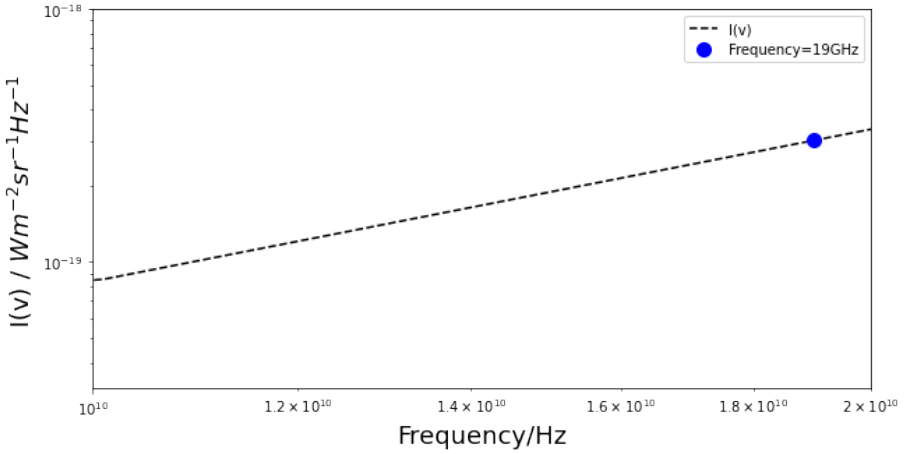

Figure 3: This is the I_v plot for linear approximation of Plank's Law. As shown in this figure, the 19 GHz with 2.725K body temperature lies on the line, indicating that it satisfies the linear approximation of Plank's Law.

1.3 Functions of Apparatus

A radiometer is used to measure the cosmic microwave background radiation in this experiment. According to the radiometer tutorials, it is a receiver that measures the average power of signals at a certain frequency interval (see [2]). Specifically, the radiometer used in this experiment is designed to measure the 19 GHz radiation in the sky. A typical radiometer composes four major components: a bandpass filter, square-law detector, integrator, and a power meter. Because the CMB signal without amplifying its magnitude is too small to be measured, an LNB amplifier is added to the radiometer in this experiment.

1.3.1 Low Noise Block Down-converter

The LNB is the first electronics connected to the horn antenna, as shown in Fig 4. It consists of an RF amplifier, an IF amplifier, and a bandpass filter to process the signal it reads from the horn antenna. The RF amplifier amplifies the 19GHz signal captured by the antenna. Its output signal is mixed with the local oscillator in the LNB to down-convert the signal to an intermediate band frequency, IF. Then the signal is amplified by the IF amplifier to output to the bandpass filter.

1.3.2 Bias-tee DC Supply

An amplifier cannot amplify the signal without any external power supply, which contradicts the conservation of energy. Therefore, a Bias-tee DC supply is connected to the LNB, as shown in Fig 4. It powers the LNB by adding a DC voltage to the AC signal and feeding it back to the LNB to operate.

1.3.3 High Pass & Low Pass Filters

A 1500 MHz low pass filter and a 1000MHz high pass filter are connected after the Bias-tee DC supply. Combining these two filters serves as a bandpass filter mentioned in section 1.3.1. This particular high pass and low pass filter configuration filters out a 500 MHz interval signal and transmit it to a power sensor.

1.3.4 Power Sensor & Power Meter

As mentioned in section 1.3, a square law detector and an integrator are required to convert the AC signal back to DC voltage proportional to microwave power. In this experiment, an HP 8481D power sensor is connected after the bandpass filter to output a DC voltage proportional to microwave power and also serves as an integrator to smooth the output voltage. The power meter is connected to the power sensor, as shown in Fig 4, to measure the output voltage and convert it back to display power.

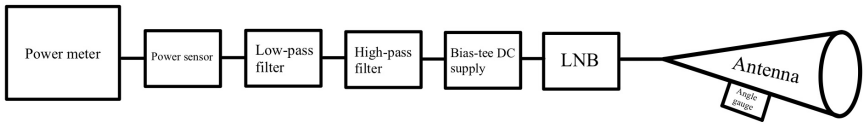

Figure 4: This is the simplified signal processing in a radiometer. The signal received by the antenna is first fed into the LNB to down-convert the signal to an intermediate frequency and amplify it. The Bias-tee DC supply is attached to the LNB to feed it with a DC voltage to power it to operate. Then, the signal goes through the low-pass and a high-pass filter, which filters out a 500 MHz frequency interval. A square-law detector catches this signal to convert the AC signal to a DC voltage proportional to microwave power. Finally, the power meter obtains the voltage and converts it back to power.

2 Experimental Procedure

2.1 Horn Antenna Pattern

Before getting into the cosmic microwave background measurement, it is necessary to investigate the characteristics of the horn antenna because different types of antennas have different beam patterns. In the cosmic microwave background measurement, it is assumed that the horn antenna is pointing at an isolated piece of the sky. Therefore, measuring the range of angles at which a horn antenna can receive the signal is needed to test this assumption

2.1.1 Apparatus Setup

Two identical radiometers are used in this experiment. One is a transmitter generating power less than 10mW placed on the Roessler Hall's balcony, and the other is a receiver placed on the roof of the Physics Building, shown in Fig 5. In this way, Two radiometers are located at a far distance, and the signal is intense enough to be measured. Inevitably, the LNB adds noise to the power measurement. Nevertheless, the LNB noise does not contribute much to the measurement in this experiment because the objective is to measure the maximum power and power ratio at different angles.

$$Power_{ratio} = \frac{Power_{\theta} - Power_{noise}}{Power_{max} - Power_{noise}} \tag{4}$$

The LNB noise shows up in both the numerator and denominator. As a result, the noise is mostly canceled in the dividing process.

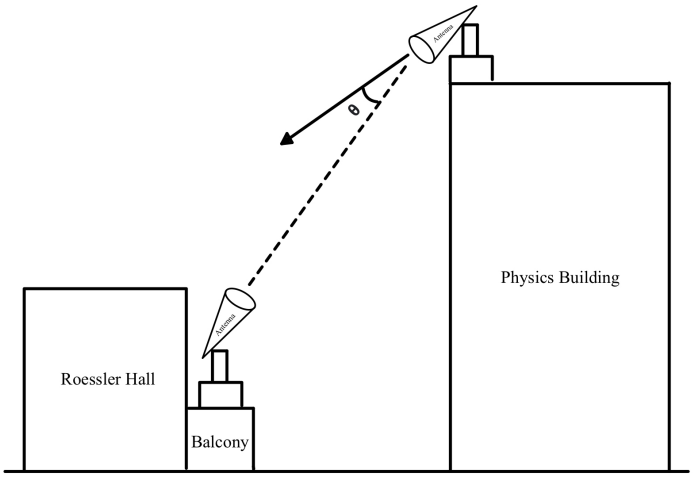

Figure 5: The transmitter was placed on the Roessler Hall's balcony, as shown on the left side. On the right side, a receiver was placed on the edge of the Physics Building. The angle was zeroed as the receiver was pointed at the center of the transmitter. The maximum range chosen in this experiment was from 0 to 90 degrees.

2.1.2 Data Acquisition

In the experiment, the receiver's horn was rotated around until the power reading on the power meter stopped increasing, indicating that the maximum power was reached. The range of angles chosen was from 0 to 90 degrees, and the starting angle was zeroed at the maximum power. To achieve better precision, each measurement was incremented by 1 degree from 0 to 60 degrees and by 2

degrees from 60 to 90 degrees. There are 76 data points recorded for each trial and 2 trials in total. The data for the first trial is shown in Table 1 in section 3.1. The rest of the data resides in /CMB data/TwoHornPattern on google drive.

2.2 Cosmic Microwave Background Measurement

This experiment was conducted outdoors on the Physics building's roof to avoid potential signal reflection due to the surrounding buildings. Also, in this way, the horn antenna can directly receive the 19GHz radiation from the sky without any physical obstacles in between, such as windows or roofs. However, putting the radiometer outdoors causes it to be exposed to a temperature-varying environment. The temperature of the equipment can shift a lot due to exposure to sunshine and wind.

2.2.1 Temperature Monitoring

Temperature measurement and their fluctuations fundamentally determine the analysis of the CMB temperature. The calculation for LNB's gain is based on the temperature of warm and cold load, as shown in Eqn 6. Also, LNB's temperature is needed to correct the gain drift in the data analysis because the shift in temperature of LNB causes variation in LNB's gain, as shown in Fig 10. Together with the LNB's gain and warm/cold load temperatures given, the CMB temperature can be estimated from Eqn 4 and 7.

Therefore, four temperatures were tracked using a digital thermometer: temperature of cold load, warm load, horn antenna, and LNB. The cold load is an EcoSorb immersed in the liquid nitrogen, which has a temperature of around 77K, and the warm load is an EcoSorb with a room temperature of around 297K. Moreover, the temperature of LNB is slightly lower than the room temperature, roughly 283K. The horn antenna's temperature was staying around 296K during the experiment, indicating that the horn antenna worked within a constant temperature range during the experiment. The temperature data for the first trial is shown in Table 2 in section 3.2.

2.2.2 Apparatus Setup

In the experiment, the radiometer was placed on the edge of the Physics Building roof. The angle of the horn antenna was zeroed using an angle gauge at the zenith point, as shown in Fig 6. The temperatures of cold load, warm load, horn antenna, and LNB were measured on the digital thermometer, and the power received was measured using the power meter. The warm and cold loads were used to calibrate the gain of the LNB. In doing so, the horn antenna was pointed to the warm and cold loads separately at the beginning of each trial.

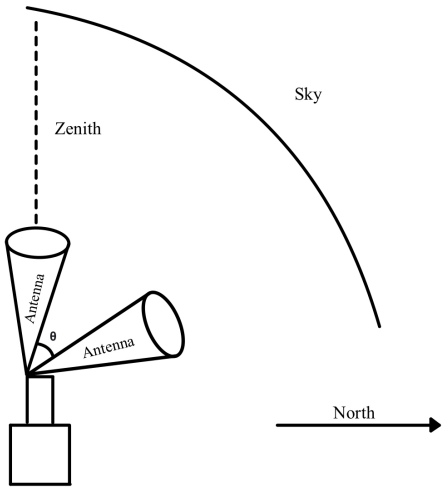

Figure 6: This is the radiometer setup for the CMB temperature measurement. The angle was zeroed at the zenith point, and the horn antenna was rotated to point to the north. The maximum angle reached was 70 degrees. Dip angles larger than 70 degrees were avoided due to the potential ground radiation interference and signal reflected by nearby buildings.

2.2.3 Data Acquisition

The experiment started with pointing the horn antenna at the zenith point, which was already zeroed. To avoid the potential signal reflection and ground radiation at larger angle, the range of angles chosen was from 0 to 70 degrees, ensuring the horn at the maximum angle does not point at the nearby building and the radiation from the ground is negligible, as shown in Fig 7. The angle measurement was not incremented by a constant degree. There were seven data points recorded in each trial with increment steps from 5 to 20 degrees. The power output, including its error, and temperatures were recorded at each angle. The data for the first trial is shown in Table 2 in section 3.2, and the rest of the 4 trials of data reside in /CMB data/CMB_measurement on google drive.

3 Data Analysis and Results

3.1 Horn Antenna Pattern Analysis

3.1.1 Measurement Data

The following table is the data recording for the first trial, showing an inverse relationship between the angle and power in general. As discussed in section 2.1.2, the angle was zeroed at the maximum power.

Angle/°	Power/mW	Angle/°	Power/mW	Angle/°	Power/mW
0	5.29	27.05	0.00823	54.00	0.000265
1.05	5.11	28.05	0.00633	55.05	0.000395
2.00	4.55	29.00	0.00284	56.00	0.000548
3.00	3.74	30.00	0.00131	57.00	0.000134
4.00	2.17	31.00	0.00285	58.00	0.000888
4.90	1.13	32.00	0.00513	59.05	0.000962
6.00	0.311	33.00	0.00541	60.00	0.000916
7.05	0.083	34.05	0.00349	62.00	0.000635
8.00	0.0876	35.05	0.00168	64.00	0.000310
9.00	0.0419	36.05	0.00175	66.05	0.000288
10.05	0.118	37.00	0.00218	68.05	0.000521
11.00	0.131	38.00	0.00395	70.05	0.000742
12.00	0.111	39.00	0.00328	72.00	0.000757
13.00	0.0681	40.05	0.00162	74.05	0.000577
14.00	0.0405	41.00	0.000685	76.05	0.000436
15.05	0.0404	42.05	0.000674	78.00	0.000292
16.00	0.0519	43.05	0.00144	80.05	0.000185
17.05	0.0503	44.00	0.00194	82.05	0.000232
18.00	0.0314	45.00	0.00180	84.00	0.000234
19.00	0.0152	46.00	0.00122	86.05	0.000280
20.05	0.0109	47.00	0.000660	88.05	0.000248
21.00	0.0146	48.00	0.000635	90.00	0.000256
22.05	0.0160	49.05	0.000875		
23.00	0.0114	50.00	0.00102		
24.05	0.00424	51.00	0.000959		
25.00	0.00273	52.00	0.000768		
26.00	0.00592	53.00	0.000355		

Table 1: This table shows the horn antenna pattern measurement data in the first trial. Power measurements were all converted to mW, and angles were measured in degrees. The rest of the data set resides in CMB data/TwoHornPattern.

The noise in the experiment was measured by turning off the transmitter and rotating the receiver's horn around to detect the background signal from the surrounding. As a result, the noise has a magnitude of 340nW. Each power value is converted into a ratio by subtracting 0.00034 mW and dividing by the maximum power, (5.29- 0.00034) mW. Moreover, the $Power_{ratio}$ is transformed into dB, shown in Eqn 5, to investigate the beam pattern.

$$Power/dB = 10 * log_{10}(Power_{ratio}) \tag{5}$$

3.1.2 Error Bar Analysis

Fig 7 and Fig 8 show the beam pattern in two trials. Nevertheless, the error bar for angles above 40° is much larger than that of angles below 40 °.

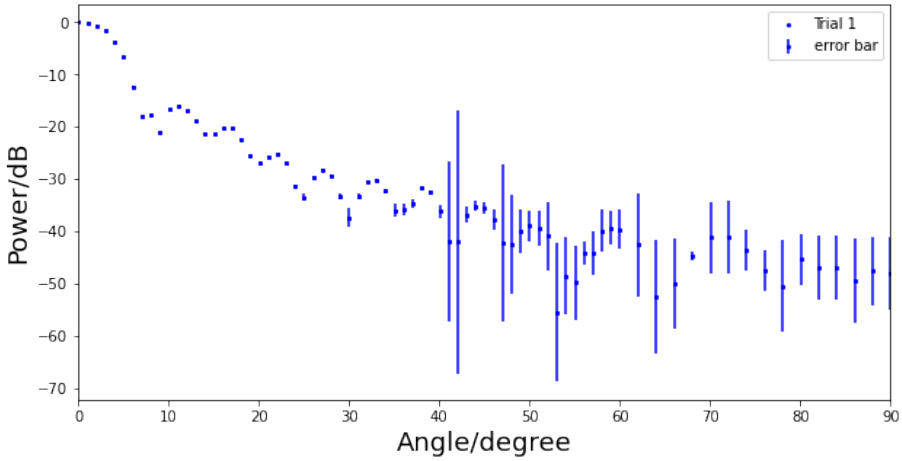

Figure 7: The beam pattern in the first trial. The plot shows that the data points above 40 degrees are noisy, and error bars are much larger than the smaller angles. Error bars for each data point are marked by blue bars.

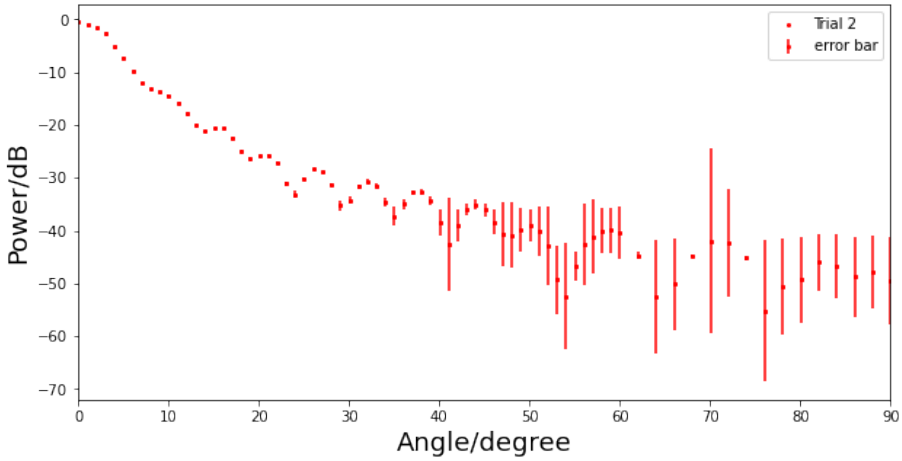

Figure 8: The beam pattern in the second trial. The plot shows a similar pattern to the first trial. Error bars for each data point are marked by red bars. Nevertheless, the data points above 40 degrees are still noisy, and error bars are much larger than the smaller angles.

Therefore, the angles above 40° is re-binned to reduce the error bar size by $\sqrt{binsize}$, as shown in Fig 9.

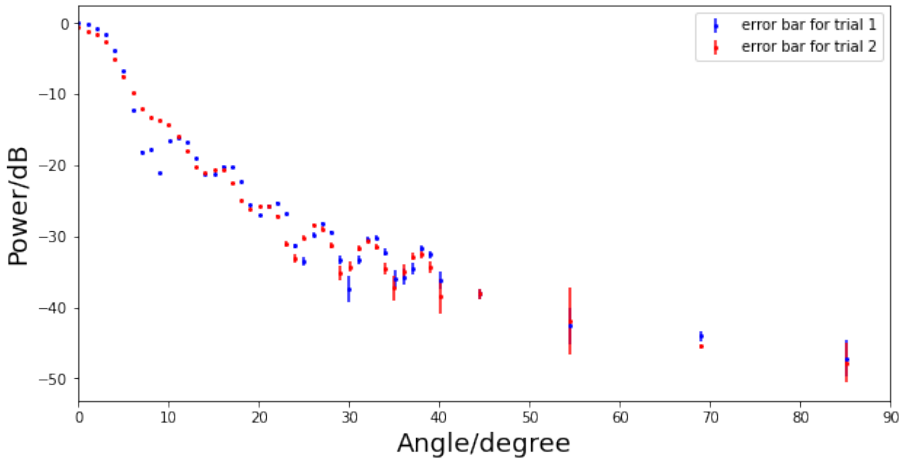

Figure 9: This plot combines the beam pattern for both trials. The angles above 40 degrees are re-binned with a bin size of 10 degrees. As shown on the right side, the size of error bars has significantly decreased. The amplitude drops to -50 dB at the largest angle.

In Figure 9, the amplitude of the signal drops to -20dB when the angle reaches 10°, meaning that the horn antenna can effectively receive the signal within 10 °, the signal's relative angle to the horn larger than 10° decreases significantly. As a result, the horn antenna can measure an approximately isolated area within 10° in the sky.

3.2 Cosmic Microwave Background Measurement Analysis

3.2.1 Measurement Data

There are five trials for cosmic microwave background measurement in total. The following table is the data recording for the first trial. The first row in the table is data for cold load calibration, marked by blue, and the second row is data for warm load calibration, marked by red.

Angle/°	T_{cold}/K	T_{warm}/K	T_{Horn}/K	T_{LNB}/K	Power/μW
-	77.549	-	296.07	283.33	1.28 ±0.1
-	-	296.57	295.88	283.42	0.649 ±0.001
0	77.552	296.61	296.45	283.27	0.474 ±0.001
5.5	77.554	296.87	295.68	283.16	0.475 ±0.002
20.5	77.550	296.89	295.44	282.93	0.477 ±0.002
40.6	77.549	296.90	296.39	283.04	0.486 ±0.002
50.7	77.548	297.03	296.12	283.20	0.496 ±0.001
60.1	77.548	297.25	296.42	283.32	0.512 ±0.001
70.5	77.549	297.51	296.28	283.54	0.547 ±0.002

Table 2: This table shows the cosmic microwave background measurement data in the first trial. Power measurements were all converted to μW, and temperatures were measured in Kelvins. The rest of the data set resides in CMB data/CMB measurement.

3.2.2 Physics Derivation

In deriving the CMB temperature from the table, it is necessary to calculate the gain of the LNB first. Nevertheless, the LNB amplifies not only the signal but also adds noise. It is shown in Eqn 6, where P_{obs} refers to the power output by the powermeter, and T_{obs} refers to the temperature the horn antenna observes.

$$P_{obs} = G(T_{obs} + T_{rec}) \tag{6}$$

T_{rec} refers to the noise the LNB amplifies, which can not be directly measured in the experiment. Its calculation involves the temperatures and powers of the cold and warm loads, shown in Eqn 7.

$$T_{rec} = \frac{T_w P_c - T_c P_w}{P_w - P_c} \tag{7}$$

T_{obs} becomes T_w as the antenna horn points at the warm load.

$$T_{obs} = T_w \tag{8}$$

Combining Eqn 6, Eqn 7, and Eqn 8, the gain equation simplifies to an equation that depends on the temperatures and power of the warm and cold load, shown in Eqn 9.

$$G = \frac{P_c - P_w}{T_c - T_w} \tag{9}$$

The variables P_{obs}, P_w, P_c , T_w, and T_c are recorded in the table. Therefore, G and T_{obs} can be calculated, and their relationship can be further simplified with Eqn 3.

$$T_{obs} = \frac{P_{obs}}{G} - T_{rec} \tag{10}$$

Furthermore, a linear relationship between T_{obs} and T_{cmb} is applied to separate the cosmic background from T_{obs}, shown in Eqn 11, where T_{cmb} is the CMB temperature, and T_A*airmass is the atmospheric noise.

$$T_{obs} = T_{cmb} + T_A * airmass \tag{11}$$

airmass is not the actual sum of air molecular mass that the horn antenna observes. In this case, the *airmass* is a relative ratio. *airmass*=1 when the horn antenna points at the zenith. The *airmass* at angle θ is given by the trigonometry equation.

$$airmass_\theta = \frac{airmass_0}{cos(\theta)} = \frac{1}{cos(\theta)} \tag{12}$$

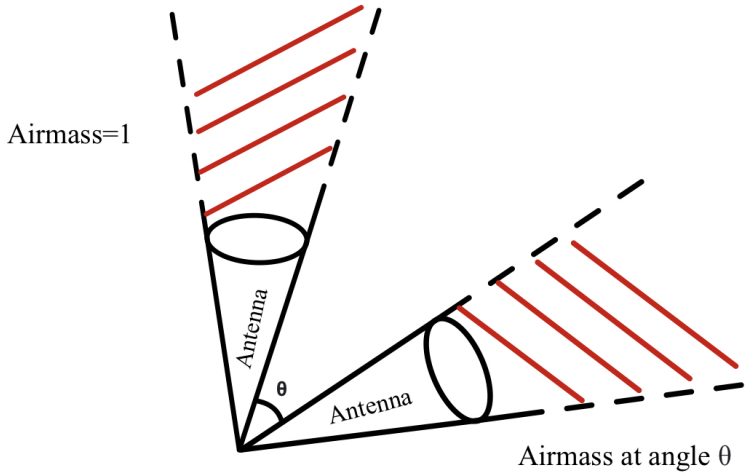

Figure 10: The airmass at the zenith point was used as the reference mass level. As the horn antenna rotates to different angles, the airmass was calculated by estimating the area ratio of the horn measures. The area ratio follows a simple trigonometry equation which equals $1/cos(\theta)$

Based on Eqn 8, $T_{obs} = T_{cmb}$ as the *airmass* approaches 0. However, in reality, *airmass*=0 cannot be directly measured. In Eqn 13, *airmass* is defined as x, and T_{obs} is defined as y, which can be described using a linear line fit. The intercept of the y axis is the cosmic background temperature by extrapolating the line fit.

$$y = T_{cmb} + T_A * x \tag{13}$$

3.2.3 Linear Line Fit Analysis

The linear line fit model with calculated T_{obs} and *airmass* values is shown in Fig 11.

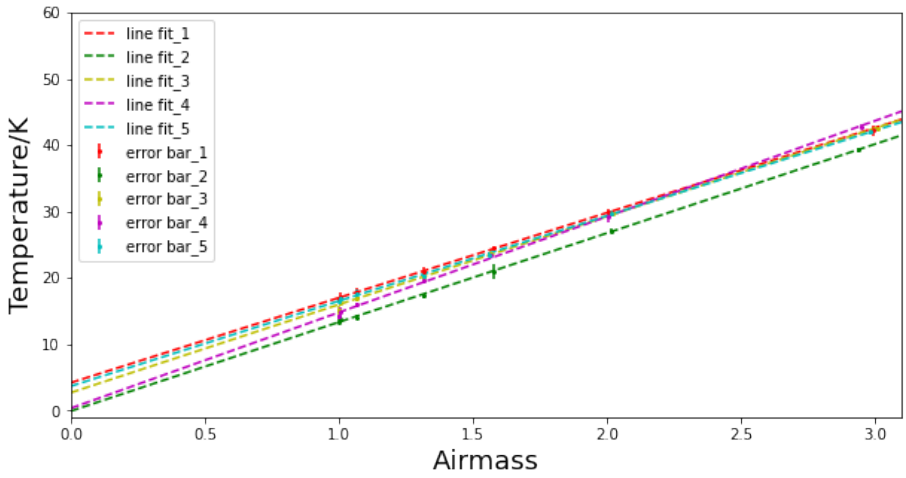

Figure 11: This plot shows the linear line fit for estimating the relationship between temperature and airmass in different trials with original data. The purple line indicates the best line fit for trial 4, which has an inconsistent slope compared to the other four trials. This inconsistency is potentially caused by the overlooked LNB gain variation, which will be discussed in sections 3.2.4 and 3.2.5.

Trial	CMB temperature/K	$T_A(slope)$	Reduced χ^2
1	4.20 ± 0.52	12.8 ± 0.3	0.15
2	-0.079 ± 0.35	13.4 ± 0.2	0.29
3	2.67 ± 0.37	13.3 ± 0.2	0.40
4	0.35 ± 0.38	14.4 ± 0.2	1.2
5	3.67 ± 0.36	12.8 ± 0.2	0.37

Table 3: This table contains the parameters and their errors from the line fits without the correction for the LNB gain. The CMB temperature varies from -0.079K to 4.20K, the slope stays around 13 except for trial 4, and the reduced χ^2 ranges from 0.15 to 1.2.

As shown in Table 3, trials 1, 3, and 5 have a relatively consistent CMB temperature, ranging from 2 to 4K, compared to trials 2 and 4. The CMB temperature even falls below the absolute zero temperature in trail 2. The potential reason for this considerable temperature variance is mentioned in section 2.2.1: the LNB gain was not constant in each trial. This line fit does not capture the

LNB gain variation.

3.2.4 LNB Gain Drift

Although it is shown in Eqn 9 that the gain is calculated from the temperature and power of warm/cold load, the LNB gain is also a function of T_{LNB}. Therefore, the gain equation needs to be corrected with LNB temperature variation.

The data file used to drive the LNB gain versus temperature relation is stored as LNB_gain_temp.txt on the PHY 122B website (see [4]). The line fit is shown in Fig 12.

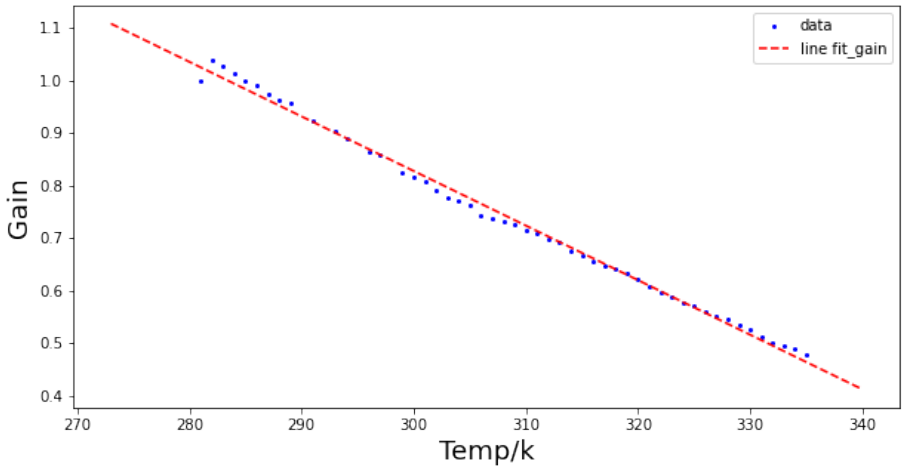

Figure 12: This plot shows the linear line fit for LNB's gain variation versus temperature based on the data provided on the PHY 112B website. The y axis indicates the relative gain ratio, and its reference level is based on T=280K. The line fit has a slope of -0.01, and it is used in Eqn 14 to correct the gain drift.

The T_{LNB} in the beginning of the experiment is set as the reference level. The temperature shifts in LNB compared to the reference level is corrected using Eqn 14.

$$G = (-0.01 * \Delta T + 1) * G \tag{14}$$

As shown in Table 4, The LNB gain fluctuates with different T_{LNB} temperatures. The line fit with corrected gains is shown in Fig 13.

T_{LNB}/K	G/90dB	ΔT/K	$G_{corrected}$/90dB
283.27	2.883	0.00	2.883
283.16	2.883	-0.11	2.885
282.93	2.883	0.66	2.892
283.09	2.883	-0.18	2.888
283.20	2.883	-0.07	2.884
283.32	2.883	0.05	2.881
283.54	2.883	0.27	2.874

Table 4: The second left column shows the constant gain that was used in the line fit shown in Fig 11. The third left column contains the LNB temperature variation compared to the reference temperature level (283.27K). Lastly, the right column shows the corrected gain value based on Eqn 14.

3.2.5 CMB Results

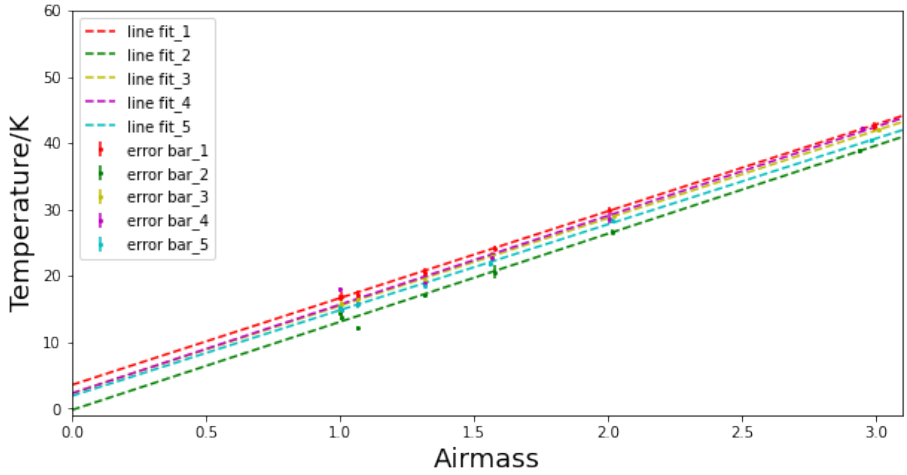

Figure 13: This plot shows the linear line fits with the corrected LNB gain. The line fit of trial 4 now has a consistent slope compared to the other four trials. However, the reduced χ^2 for this fit jumps from 1.2 to 11.6. This will be addressed in section 4.2.

As shown in Fig 13, all line fits exhibit a parallel trend with the corrected LNB gain. Their slopes are consistent and stay around 13, while the slopes in the last line fits fluctuate a lot, ranging from 12 to 14, as shown in Table 3. This improvement indicates that the correction of LNB gain drift eliminates the unobserved bias in measurement data due to the constant G value. All parameters and their errors are shown in Table 5.

Trial	CMB temperature/K	$T_A(slope)$	Reduced χ^2
1	3.70 ± 0.52	13.1 ± 0.32	0.16
2	-0.079 ± 0.36	13.2 ± 0.20	8.5
3	2.44 ± 0.37	13.1 ± 0.21	0.34
4	2.43 ± 0.38	13.3 ± 0.22	11.6
5	2.03 ± 0.36	12.8 ± 0.20	0.73

Table 5: This table includes the parameters and their errors from line fits with the corrected LNB gain. The CMB temperature varies from -0.079K to 3.70K, the slopes stay around 13, and the reduced χ^2 ranges from 0.15 to 11.6, which increased a lot compared to Table 3.

As shown in Table 5, all trials have relatively consistent CMB temperatures compared to Table 3. However, the reduced χ^2 values are abnormal. Especially, the χ^2 in trial 4 significantly increases from 1.2 to 11.6. This deviant χ^2 behavior will be further discussed in section 4.2. The CMB temperature value is calculated by inversely weighting their uncertainties. Moreover, the statistical uncertainty is estimated by error propagation. The CMB temperature value with its statistical uncertainty is shown below.

$$T_{cmb} = 1.7K \pm 0.4K(stat) \tag{15}$$

3.3 Sources of Systematic Errors

Nevertheless, this experiment has systematic errors that are not counted in the previous analysis. There is number of factors can potentially cause systematic errors.

3.3.1 Air Humidity

The H_2O molecules in the air can emit a radio noise which the horn antenna can also receive. If the air humidity varied a lot during the experiment, the signal received would contain noises with different magnitudes. As a result, the T_{obs} values are impacted in an unknown way, contributing to the measurement errors. However, the humidity remains constant at 20 % according to data provided on UC Davis Atmospheric Science's website (see [3]). Thus, air humidity did not generate significant systematic errors in the experiment.

3.3.2 Ground Radiation

There is also radiation coming from the ground that the horn antenna can detect if the dip angle is larger enough. Specifically, in this experiment, the largest dip angle was 70°, which is still (90°-70°)=20° away from the ground. As shown in Fig 9, the ground radiation attenuates to -30dB. Therefore, it does not contribute much noise to the power output.

3.3.3 Cold Load Temperature Bias

The primary systematic error comes from the temperature measurement of the cold load. The cold load is an EcoSorb immersed in the liquid nitrogen inside a box. As time elapses, the liquid nitrogen evaporates, causing the EcoSorb is no longer fully immersed in the liquid nitrogen. The top part of the EcoSorb's temperature is different from the bottom part's temperature.

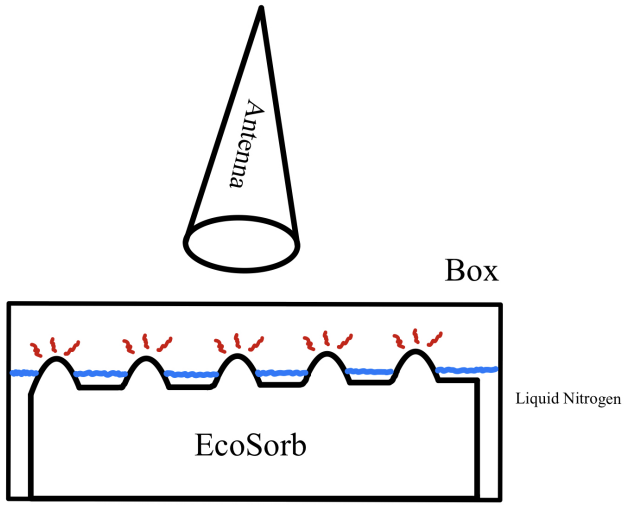

Figure 14: The horn antenna was pointed at the cold load and measured the temperature of the cold load. As shown in the graph, the top part of the Ecosord was already out of liquid nitrogen. Therefore, the temperature of the top part is higher than the bottom part. However, the horn antenna captured the hot top part while the thermometer did not. This created a measurement bias that the actual temperature of the cold load is underestimated, as described in Eqn 16.

In the calibration process, the horn antenna observed the temperature of the whole cold load, including the top and bottom parts of the EcoSorb while the thermometer mainly measured the part immersed in the liquid nitrogen. As a result, the measured temperature did not account for the temperature difference in the EcoSorb. Therefore, the temperature used for calibration underestimates the actual temperature.

The estimated temperature difference is +2K. This estimation comes from comparing the T_{cmb} value between the first trial and the last trial. The Ecosorb was fully immersed in the liquid nitrogen in the first trial. The time interval between the two trials was 30 minutes, enough for liquid nitrogen to evaporate. The T_{cmb} value in the last trial should be approximately equal to the T_{cmb} value

in the first trial, with all else being equal. However, the T_{cmb} difference is 1.7K. The assumption is that underestimating the cold load changes the gain in the last trial, as shown in Eqn 16. ΔT= 2K is an estimated value which makes $T_{cmb1} \approx T_{cmb5}$ by changing the G value in Eqn 16.

$$G = \frac{P_c - P_w}{(T_c + \Delta T) - T_w} \tag{16}$$

The line fit accounting for the systematic errors is shown in Fig 15, and all parameters and their errors are shown in Table 5.

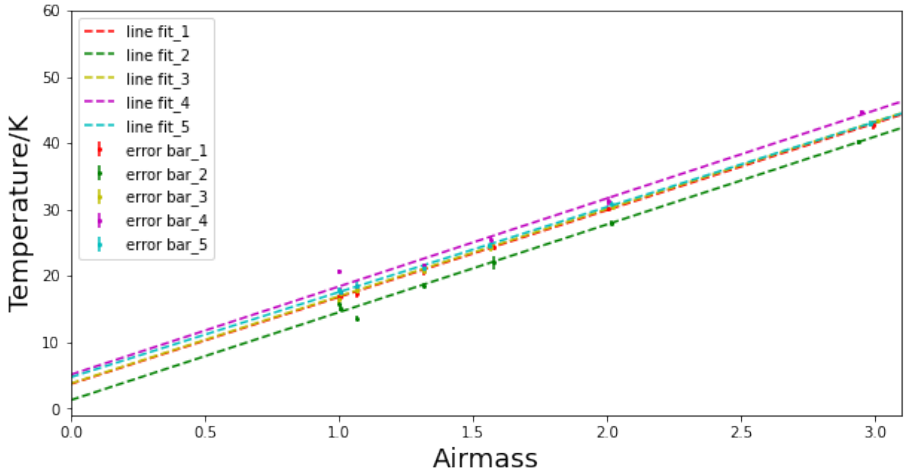

Figure 15: This plot shows the linear line fits with corrected T_{cold}. The line fits have shifted upward by approximately 1 to 2K. The CMB temperature for trial 2 was negative in the previous line fits, which is impossible because temperatures below absolute zero degrees are not reachable. However, by correcting this temperature bias, the intercept for trial 2 increased from a negative temperature to a positive temperature.

Trial	CMB temperature/K	T$_A$(*slope*)	Reduced χ^2
1	3.7 ± 0.52	13.1 ± 0.32	0.16
2	1.3 ± 0.36	13.2 ± 0.20	8.5
3	3.8 ± 0.37	13.1 ± 0.21	0.34
4	4.4 ± 0.38	13.3 ± 0.22	11.6
5	4.1 ± 0.36	12.8 ± 0.20	0.73

Table 6: This table incorporates the parameters and their errors from line fits with the corrected LNB gain and the systematic errors from temperature measurement. The CMB temperature varies from 1.3K to 4.4K. The slopes and the reduced χ^2 are unchanged compared to Table 5. It seems reasonable because this temperature measurement bias shifts the line fit upward.

The CMB temperature value with systematic error is calculated from Table 5 by inversely weighting their uncertainties. The systematic error is estimated by subtracting this value from T_{cmb} in Eqn 14. As a result, the calculated CMB temperature systematic error is 1.3K, and the final result with statistical and systematic errors is shown below.

$$T_{cmb} = 1.7K \pm 0.4K(stat) \pm 1.3K(syst) \tag{17}$$

4 Discussion

The CMB temperature is 1K smaller than the expected value, 2.725K. However, this is an acceptable value because the T_{cmb}=2.725K falls within the range of the measurement values including the statistical and systematic errors. Therefore, there is still room to improve the accuracy and precision of the measured T_{cmb} value by reducing statistical and systematic errors. In this experiment, the systematic error, 1.3K, is almost as large as the measurement value. This is because a slight temperature difference in measuring the cold temperature contributes to a considerable change in the T_{cmb}. The simplest way to avoid this situation is to prepare adequate liquid nitrogen so that the EcoSorb can be fully immersed for hours during the experiment. Besides this, many other potential factors can also improve the accuracy and precision of the measurement result in the following subsections.

4.1 LNB Gain Data Accuracy

As shown in Fig 12, there is an outlier that deviates from the line fit around 280K. However, the temperature range of LNB used in this experiment was also around 283-284K. In other words, if measurement errors caused this outlier, it would impact the value of the corrected gain in Eqn 14. As a result, the gain was corrected based on the faulty dataset, making the gain value even more inaccurate. Moreover, it is not explicitly stated that the LNB used in the experiment is identical to the one used in the gain vs. temperature measurement. It is not guaranteed that each LNB had exactly the same characteristic when they were produced. Therefore, the data file used for correcting the LNB gain is not trustworthy. If more time was available, the LNB gain vs. temperature relationship needs to be tested using the actual LNB in the experiment.

4.2 Abnormal Reduced χ^2 Values

As shown in Table 3 and Table 5, the reduced χ^2 values had significantly increased from 1.2 to 11.6 in trial four and from 0.3 to 8.5 in trial two when the LNB temperature variation corrected the gain. This is because the T_{obs} is no longer only dependent on the airmass, as shown in the Eqn 11, but it also inexplicitly depends on the ΔT_{LNB} variation, which determines the gain value. As a result, a linear line fit may not be a good line fit to describe this

model, causing poor goodness of fit. In this way, the increased reduced χ^2 values suggest an incorrect line fit is applied. However, another explanation is that the data points are insufficient to give an optimal reduced χ^2 value. In each trial, only seven data points were used; one outlier would shift the reduced χ^2 value by a considerable amount. It is possible that the reduced χ^2 would approach one if more data points were measured.

4.3 Experiments on the Experiment

The horn antenna's vertical angle range was measured from 0 to 70 degrees, and the horizontal angle of the horn antenna was assumed to point to the north. However, the horizontal angle of the horn antenna was not measured in this experiment. The horn antenna was roughly pointed to the north in each trial. Therefore, it is possible that the horizontal angle of the horn antenna varied from trial to trial, and this effect on CMB temperatures was not examined in the analysis. The horn antenna with different horizontal angles could measure the signal with various amplitudes at the same vertical angle. Additional experiments need to be conducted to test the relationship between the amplitude of the signal received and the horizontal angle of the horn antenna. In this way, the effect of measuring signals at different horizontal angles can be isolated in the analysis.

5 Conclusion

This experiment aims to measure the cosmic microwave background originating from the universe's beginning. The measurement result is 1.7K $\pm$ 0.4(stat) $\pm$ 1.3(syst), which is about 1 K different from the published value, 2.725K. Despite the difference in magnitude, this result validates the existence of cosmic microwave background in the universe. In this experiment, electronics such as low-pass filter, high-pass filter, and amplifier are applied to measure a weak signal from a distant place. Furthermore, in the data analysis part, CMB temperature is affected by several factors. For example, the gain of the LNB drifts with temperature, and the temperature of the cold load is underestimated. It is essential to identify these systematic errors to acquire an accurate and precise result.

6 Acknowledgments

Acknowledging the help of lab partner, Brooke Schuld, who had been helpful and showed great teamwork during the experiment.

References

[1] T. Tyson, B. Barnett, S. Hillbrand, April 2019, Measurement of the Cosmic Microwave Background Radiation at 19 GHz.

[2] Radiometers tutorial from https://122.physics.ucdavis.edu/?q=node/35.

[3] Air humidity data from http://apps.atm.ucdavis.edu/wxdata/.

[4] LNB gain data from https://122.physics.ucdavis.edu/?q=node/35.

[5] Measurement data available on https://drive.google.com/drive/folders/15M2h35Vz6eT6UqvjjYhWpkrJQGWEIJD0?usp=sharing